Int. J. Electrochem. Sci., 17 **(2022)** Article Number: 220528, doi: 10.20964/2022.05.18

International Journal of
ELECTROCHEMICAL
SCIENCE
www.electrochemsci.org

Facile Synthesis of New Conductive Hydrogels for Application in Flexible all-solid-state Supercapacitor

Guizhen Guo[1,*], *Hong Sun*[1], *Youyi Sun*[2], *Mengru Li*[2]

[1] Department of Applied Chemistry, Yuncheng University, Yuncheng 044000, PR China.
[2] School of Materials Science and Engineering, North University of China, Taiyuan 030051, P.R. China.
[*]E-mail: guoguizhen1986@163.com

Received: 27 January 2022 / *Accepted:* 1 March 2022 / *Published:* 5 April 2022

A new conductive hydrogels based on PVA/GO/SA/PANI (PGOSAP) are prepared for application in electrode of flexible supercapacitors. The conductive hydrogels exhibit excellent mechanical properties with a elongation at break of 220% and tensile strenght of 3.3 MPa. Furthermore, the flexible supercapacitor is fabricated from the conductive hydrogels have special significance in fabricating deformable. In this work, multi network structure conductive hydrogel with no deformation and has been prepared. Taking advantage of the synergistic effects of PVA and SA the hydrogel can form without crosslinker and the crystallization area of composite hydrogel smaller than that of single material, thus providing more channels for electrolyte transfer. Finally, a novel one-piece integrated flexible supercapacitor based on PGOSAP hydrogel was assembled. The results show that, there was no displacement or lamination between electrolyte and electrode after 3500 cycles. The novel one-piece integrated flexible supercapacitor with excellent mechanical properties is expected to broad prospects for fabricating deformable flexible supercapacitors.

Keywords: all-solid-state, flexible supercapacitor, polyvinyl alcohol, Sodium alginate, Graphene oxide, polyaniline

1. INTRODUCTION

Flexible all-solid-state supercapacitor has attracted lots of interesting for application in wearable device[1-3]. The whole device need to be as elastic as skin to meet the deformation stress changes caused by human joint bending[4-5]. The flexible all-solid-state supercapacitor is usually achieved by combining flexible solid-state electrodes with electrolytes. The conductive hydrogels are generally acted as electrodes of flexible all-solid-state supercapacitor due to excellent flexibility, elasticity, conductivity and electrochemical activity[6-7]. The graphene and PANI are often used to electrode materials of supercapacitor due to high conductivity and electrochemical activity[8-9]. PVA

is generally used to matrix of hydrogels due to non-toxic, non-carcinogenic and gel forming properties[9]. So, there are some works reporting the synthesis of PVA based hydrogel for application in supercapacitors. For example, Wang et al reported the synthesis of PVA-H_2SO_4 hydrogel based on glutaraldehyde and PVA by casting and scraping for application in flexible supercapacitor[10]. Then, the aniline was added to the PVA-H_2SO_4 hydrogel by the traditional immersion adsorption method, and was in-situ polymerization to form PVA/PANI hydrogel. Gao et al prepared PVA/PA hydrogel film by a simple gradual freezing/thawing method for application in supercapacitor[11]. Then, aniline and APS were added to PVA/PA hydrogel by immersion adsorption method, and was in-situ polymerization to form PVA/PA/PANI hydrogel. However, these conductive hydrogels were coated on surface of carbon or metal collector for application in supercapacitor, reducing the flexibility and elasticity of supercapacitor. In addition, it showed high interfacial resistance and low interfacial strength between conductive hydrogels and collector, restricting the improvement of electrochemical performance and mechanical stability. Therefore, compared with traditional electrode materials and collector, the hydrogel with high conductivity is highly required to simultaneously act as electrode materials and collector due to following several advantages. Firstly, it has simple structure and good mechanical flexibility. Secondly, there is no bonding interface between electrode materials and collector, reducing the risk of damage and falling off of the contact surface. Thirdly, it is high content for the active material in hydrogels, which is very beneficial to the improvement of the specific capacitance of the supercapacitor[12-14]. Previous study showed that sodium alginate combined with polyaniline could form a self-supported hydrogel with good conductivity without cross-linking agent[15]. However, the hydrogel exhibited poor flexibility due to sodium alginate (SA) with rigid property[16]. Therefore, it is a high challenge to prepare the hydrogel with high conductivity, flexibility and elasticity.

Here, a new hydrogel based on PVA/GO/SA/PANI is designed and prepared by a hydrogen bonding process for application in electrode of supercapacitor. The PVA based hydrogel mainly provided the excellent flexibility and elasticity. The GO and SA@PANI provided the good conductivity and electrochemical active performance. The work provides a new idea for design and preparation of conductive hydrogel with high performance for various applications.

2. EXPERIMENTAL

2.1 Reagents and material

Graphene oxide (GO, 2.0wt%) aqueous solution was purchased from Tangshan Jianhua Co., Ltd. Ammonium persulfate (APS), Aniline (An), sodium alginate (SA) and Polyvinyl alcohol (PVA, 99% hydrolyzed, degree of polymerization 1750) were analytical grade and purchased from Tianjin Damao Chemical Reagent Co., Ltd. H_2SO_4 (1.0 M) were analytical grade and purchased from Luoyang Haohua Chemical Reagent Co., Ltd

2.2 Preparation of conductive hydrogel

The conductive hydrogel was prepared by hydrogen bonding interaction according to following process. Firstly, 1.5 g GO was added to the 10 ml PVA solution (10wt%) under mechanical stirring and ultrasonic for 15.0 min. And then 0.2 g SA was added to the above PVA/GO solution under magnetical stirring for 2.0 h. Secondly, 0.37 g (4.0 mmol) aniline was added to the above PVA/GO/SA solution under magnetical stirring for 15.0 min. Finally, 0.91 g (4.0 mmol) of APS was dissolved in HCl (1.0 M 3.0 ml) solution and then added to the PVA/GO/SA solution under stirring. After 5.0 min, the above mixing solution turned dark green, forming PANI. After freezed at -20 ℃ for 24 hours, the PVA/GO/SA/PANI conductive hydrogel (PGOSAP) was formed. In contrast, GO/SA/PANI hydrogel without PVA was prepared by the same process (referred to as GOSAP). The hydrogels were placed in a large amount of deionized water for three days. The water was removed every 12.0 h to remove oligomers such as inorganic substances and aniline.

2.3 Preparation of supercapacitors based on PGOSAP and GOSAP hydrogel

The 1.0 g PVA was dissolved in 10 mL distilled water and then freezed at -20 ℃, forming PVA hydrogel. The PVA hydrogel was soak in 1.0 M H_2SO_4 solution for 2.0 h, forming H_2SO_4/PVA hydrogel. Here, symmetrical supercapacitor (1.0 cm×2.0 cm) with sandwich structure was fabricated by assembling method. The PVA/GO/SA/PANI conductive hydrogel was used as the collector and electrochemical active substances. The content of active material was about 2.4 mg cm^{-2}.

2.4 Characteristic measurements

The surface structure of the samples was characterized by field emission scanning electron microscopy (FE-SEM, Su-8010).

Chemical structure of the samples was characterized by Fourier transform infrared (FT-IR) spectrometer (Thermo Nicolet-6700F) in the range of 4000-400.0 cm^{-1}.

X-ray diffraction (XRD) patterns were measured on a Rigaku diffractometer (TD 3500) equipped with Cu Kα radiation (k = 0.15406 nm).

The mechanical properties of the samples were characterized by tensile and compressive tests (AI-7000-SGD).

2.5 Electrochemical performance of supercapacitor

The galvanostatic charge-discharge (GCD) profiles of supercapacitors were measured by a charge-discharge testing system (CT2001A,Wuhan,China) at the different current density within a voltage window of -0.2 to 0.8 V. The cyclic voltammetry (CV) measurements were carried out from -0.2 to 0.8 V at the different scanning rates. The electrochemical impedance spectroscopy (EIS) was conducted at varying frequency from 100 kHz to 0.01 Hz with an amplitude of 5.0 mV at an open-circuit voltage. Both CV and EIS were performed on a electrochemical workstation (CHI 660E).

Based on the data of GCD curves, the special capacitance (C_{SP}, F g^{-1}), area capacitance (C_{SA}, F cm^{-2}), Energy density (E_{SP} *or* E_{SA}, Wh Kg^{-1} or Wh cm^{-2}) and Power density (P_{SP} or P_{SA}, W Kg^{-1} or W cm^{-2}) of single electrode materials can be calculated by the following equations[15-16]:

$$C_{SP} = \frac{I_2 \Delta t}{m \Delta V} \quad \text{or} \quad C_{SA} = \frac{I_2 \Delta t}{S \Delta V} \qquad (1)$$

$$E_{SP} = \frac{C_{SP} \Delta V^2}{2 \times 3600} \quad \text{or} \quad E_{SA} = \frac{C_{SA} \Delta V^2}{2 \times 3600} \qquad (2)$$

$$P_{SP} = \frac{E_{SP} \times 3600}{\Delta t} \quad \text{or} \quad P_{SA} = \frac{E_{SA} \times 3600}{\Delta t} \qquad (3)$$

Where I_2 (A) and Δt (s) are the discharge current and the discharge time, respectively. ΔV (V) is the potential window during the discharge process excluding IR drop. m (g) and S (cm^{-2}) are the mass of active materials and area of electrode, respectively.

3. RESULT AND DISCUSSION

The formation of present conductivity hydrogel was attributed to gel properties of PVA at low temperature as shown in Fig.1A.

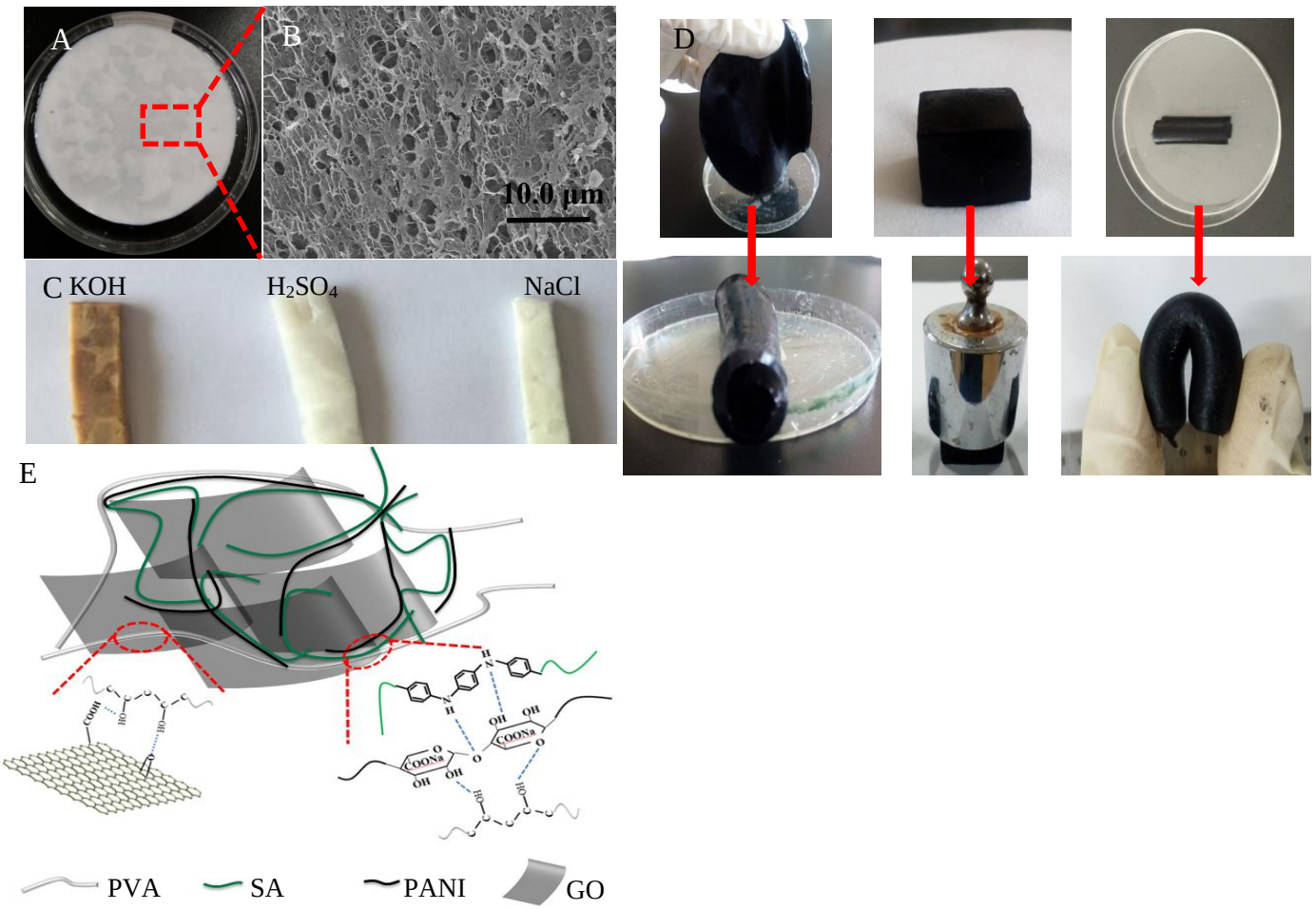

Figure 1. (A) Optical photo and (B) SEM image of PVA hydrogel, (C) Optical photos of PVA hydrogel after soaking in different electrolytes and left for one week. (D) Optical photos of PGOSAP hydrogels with different shapes and elastic deformation. (E) Schematic illustration of hydrogen bonding interaction within the system of PGOSAP hydrogels.

Furthermore, the PVA hydrogel has a three-dimensional network structure (Fig.1B), providing a large amount of space and channel for the electrolyte and ion storage. In order to sbelect suitable electrolyte, PVA hydrogel was soaked in 1.0 M KOH solution, 1.0 M H_2SO_4 solution and 1.0 M NaCl solution for 2.0 h. After being removed, it was put in a self sealing bag and stored at room temperature (Fig.1C). It was found that the PVA hydrogel showed poor stability and lose flexibility after immersion in KOH solution. Contrarily, the PVA hydrogel containing with H_2SO_4 showed mechanical stability and good flexibility. Therefore, 1.0 M H_2SO_4 solution was selected as the electrolyte. Furthermore, these active materials (eg. GO or PANI) were introduced to PVA hydrogel, which slightly affected mechanical stability and good flexibility. As shown in Fig.1D, the PGOSAP hydrogel could be fabricated to various shape by mould process. Moreover, it still showed high mechanical stability and good flexibility, which is key role for application in supercapacitor. The good mechanical stability and good flexibility were attributed to synergistic effect of SA, PVA, GO and PANI as shown in Fig.1E. It possessed dual network structure due to the large number of carboxyl and hydroxyl groups in the SA, PVA, GO and amino groups in PANI structure. One of them is the entanglement of PANI with SA and PVA molecular chains, caused by hydrogen bonding (and electrostatic) interactions. The other is hydrogen bonding within the GO and PVA chains.

The formation of PGOSAP hydrogels was further confirmed by FT-IR and X-ray diffraction spectra. Fig.2A shows the FT-IR spectra of GOSAP and PGOSAP hydrogels. The two samples showed similar FT-IR curves due to contain with same components of GO, PANI and SA. The peak at 1550 cm^{-1} was assinged to the characteristic absorption peak of C=C stretching vibration on benzene chains and quinone rings of GO and PANI. The peak at 1090 cm^{-1} was assinged to C-N absorption vibration peak in PANI[17]. The peaks at 1650 cm^{-1} and 3456 cm^{-1} were assinged to the -COO antisymmetric stretching vibration and O-H stretching vibration of SA, respectively[18]. These results indicated the formation of hydrogels with the GO, PANI and SA. Compared with GOSAP hydrogel, the absorption peaks of PGOSAP hydrogel decreased. In addition, it was found that the stretching vibration characteristic absorption peak of C-N in PANI was blue shift from 1090 cm^{-1} to 1128 cm^{-1} for the PGOSAP hydrogels comparing to GOSAP hydrogels. These results were due to the more crosslinking points in the gel after PVA addition, the stronger hydrogen bonding and intermolecular force. Fig.2B shows the XRD spectra of GOSAP and PGOSAP. The diffraction peak at $2\theta=20.5°$ was assigned to crystallization peak of PVA in PGOSAP hydrogel, indicating the formation of PVA semi crystalline region in the hydrogel. The diffraction peak at 40.7° was assigned to the order stacking degree of PVA molecular chain. The result indicates that the formation of PVA based hydrogels results from PGOSAP hydrogels, forming cross-linking points.

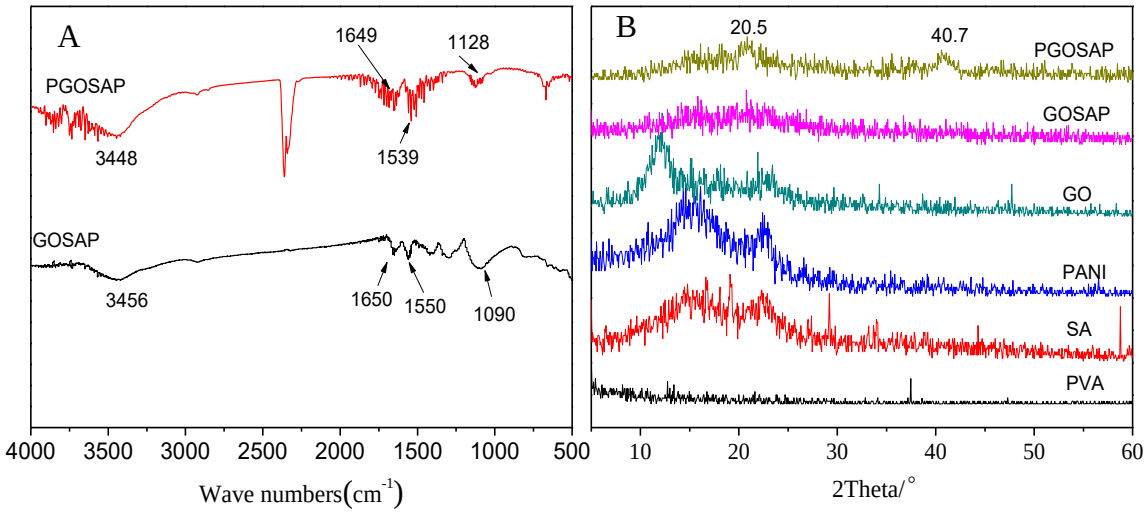

Figure 2. (A) FTIR and (B) XRD patterns of GOSAP and PGOSAP hydrogel.

The micro-structure of GOSAP and PGOSAP hydrogel was characterized by SEM images as shown in Fig.3. In order to investigate the gel structure of GOSAP and PGOSAP, the hydrogels was vacuum freeze-dried and then sprayed with gold. There were obvious phase separation in GOSAP hydrogel (Fig.3A), and many fibrous substances were attached on the lamellar structure. The PGOSAP hydrogel (Fig.3B) had a uniform microstructure, a smooth porous structure and obvious globular cross-linking sites. This structure character leaded to a high specific surface area and high water absorption capacity, facilitating the interconnection of electrolytes, the diffusion of ions and the transmission of electrons. In addition, the dense network structure and lamellar orientation were also observed due to the GO lamellar structure, enhancing the strength of PGOSAP hydrogel. The energy disperse spectroscopy (EDS) and elemental mapping images of GOSAP and PGOSAP hydrogels were also characterized as shown in Fig.3C and 3D, respectively. It can be clearly seen from the element map that the distribution of elements in the hydrogel is uniform. In addition, these C, O, N, S and Na elements were all observed for GOSAP and PGOSAP hydrogels. The result further indicated the formation of GOSAP and PGOSAP hydrogels with uniform and porous structure.

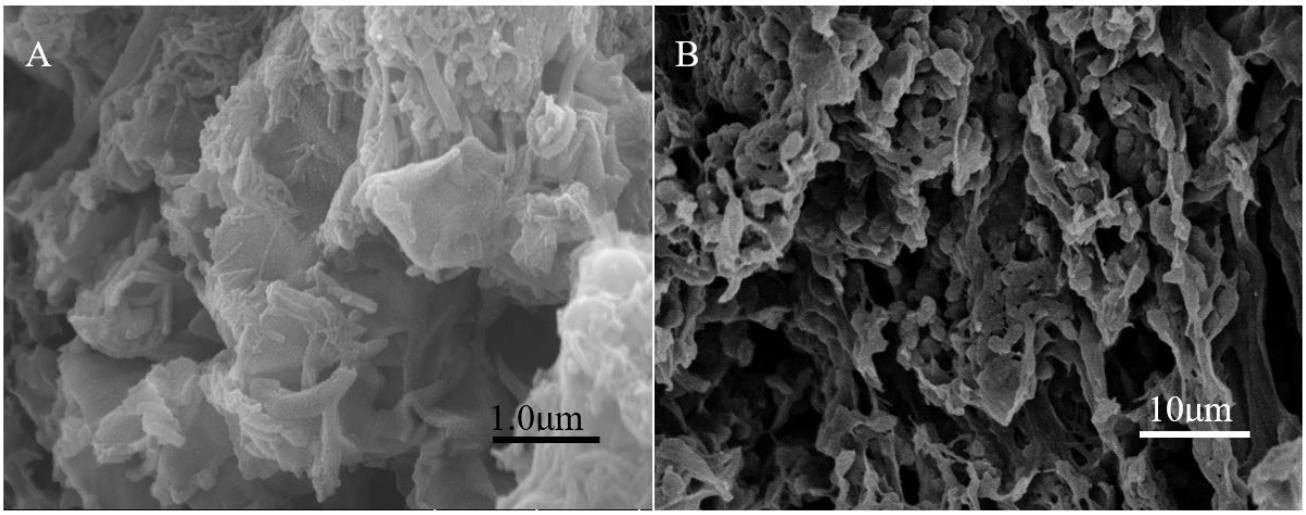

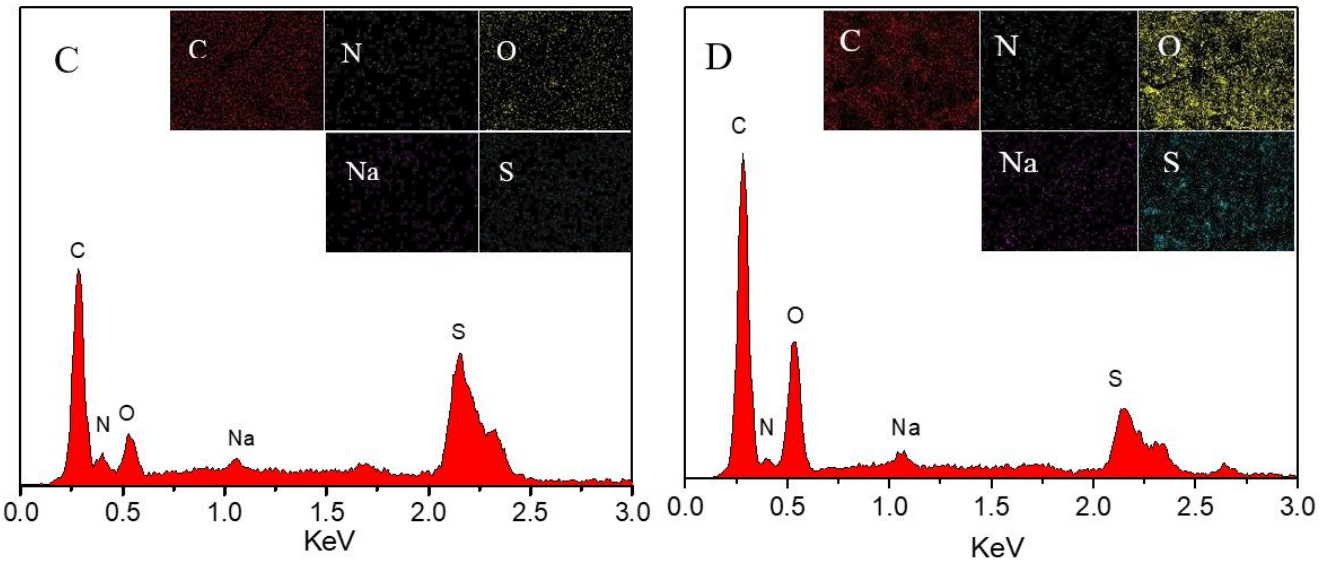

Figure 3. SEM images of (A) GOSAP hydrogel and (B) PGOSAP hydrogel. EDS spectrums and elemental mapping images of (C) GOSAP hydrogel and (D) PGOSAP hydrogel.

Fig.4A shows the tensile stress-strain curves of GOSAP and PGOSAP hydrogels. It was found that the stress-strain curves of GOSAP and PGOSAP hydrogels were high linearity before fracture. The result indicated the excellent elasticity for the GOSAP and PGOSAP hydrogels. In a comparison, the PGOSAP hydrogels showed higher mechanical strength than GOSAP hydrogels. The tensile strength of GOSAP and PGOSAP hydrogels was about 0.9 MPa and 3.3 MPa respectively. And the elongation at break of GOSAP and PGOSAP hydrogels are 123% and 220%, respectively. Fig.4B shows the compressive stress-strain curves of GOSAP and PGOSAP hydrogels. When the compression strength is 40MPa, GOSAP and PGOSAP hydrogels can be compressed to 45% and 70% respectively. The result was attributed to formation of cross-linking based on PVA crystalline region. In addition, the good flexibility and strength of PGOSAP hydrogels were also attrbiuted to the interaction of PVA and SA. The non covalent bond force between PVA molecular chains provided a certain degree of stretching and sliding ability, leading to good flexibility.

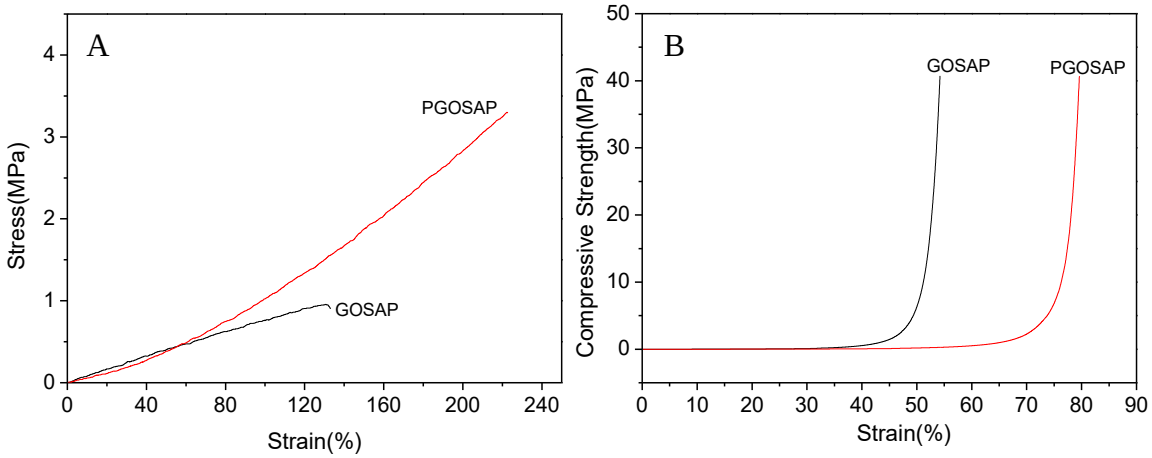

Figure 4. (A) Tensile and (B) Compression stress-stain curves of GOSAP and PGOSAP hydrogels.

The conductive performance of PGOSAP hydrogel was characterized by light bulb as shown in Fig.5. It was found that the PGOSAP hydrogel can also work as a power supply unit and light up a yellow LED under various external forces, indicating excellent conductivity. In addition, it also indicated that the mechanical deformation was few effect on its conductivity. It further showd that PGOSAP hydrogel had good electrical conductivity and mechanical stability. The good conductive performance was attributed to synergistic effect of PVA and SA. When the external force is applied on the hydrogel, the hydrogen bond between the PVA macromolecule and the SA is destroyed[19-21]. When the external force disappears, the hydrogel can restore to its original state. Therefore, the conductivity of the PGOSAP hydrogel remains few change during the stretching process.

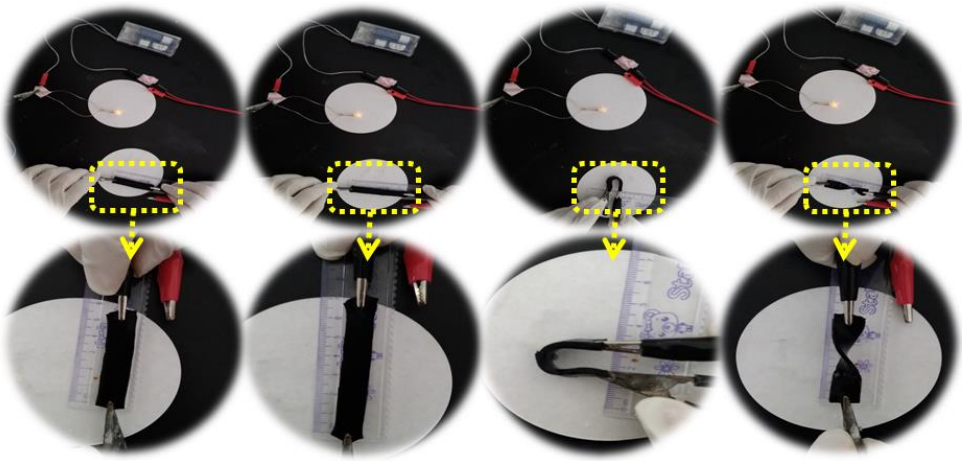

Figure 5. The photograph of PGOSAP hydrogel as a power supply unit

Fig.6 shows the CV curves of supercapacitors based on GOSAP and PGOSAP gel as a function of scanning rate (20.0~100.0 mV/s). The obtained CV curves are approximately rectangular and symmetrical. The current response increased with increasing in scanning rate. In addition, at the scanning rate, the area of the CV curve of PGOSAP hydrogel is larger than that of GOSAP hydrogel. Generally, the specific capacitance of supercapacitor is directly proportional to the area of CV[22]. The result indicated that the PGOSAP hydrogel showed larger specific capacitance comparing to GOSAP hydrogel. The result was attributed to the porous network structure and larger specific surface area of PGOSAP hydrogel, providing a high active surface area and enhancing speed electron transfer channel for charge accumulation.

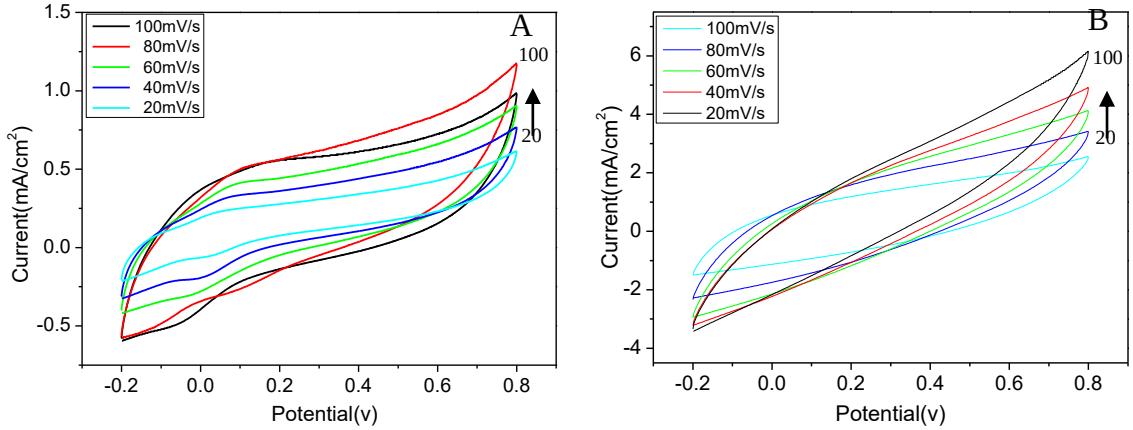

Figure 6. CV plot of supercapacitor based on (A) GOSAP and (B) PGOSAP at various scan rates of 20.0 mV/s, 40.0 mV/s, 60.0 mV/s, 80.0 mV/s and 100.0 mV/s.

Fig.7A shows GCD curves of supercapacitors based on GOSAP and PGOSAP hydrogel at a current density of 2.0 mA/cm^2. Both supercapacitors could maintain approximately linear and symmetrical charge discharge characteristics. In addition, the discharge time of supercapacitor based on PGOSAP hydrogel was significantly longer than that of supercapacitor based on GOSAP hydrogel. The result indicated that the PGOSAP hydrogel showed larger specific capacitance comparing to GOSAP hydrogel.

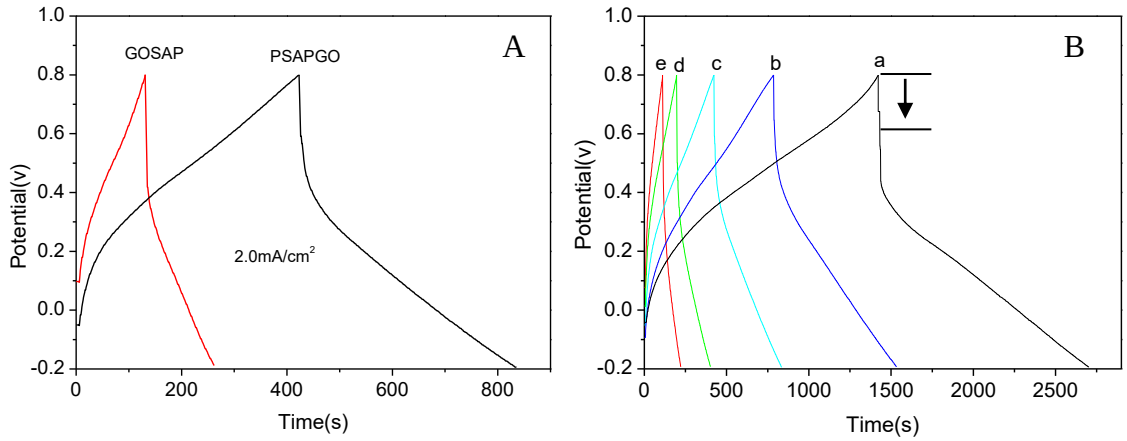

Figure 7. (A) GCD plots of supercapacitor based on GOSAP and PGOSAP. (B) GCD plots of supercapacitor based on PGOSAP at various currents of (a) 1.0 mA/cm^2, (b) 1.4 mA/cm^2, (c) 2.0 mA/cm^2, (d) 3.0 mA/cm^2 and (e) 4.0 mA/cm^2.

The specific capacitance of the supercapacitor based on GOSAP hydrogel and PGOSAP hydrogel was about 0.4 F cm^{-2} and 1.1 F cm^{-2} at the current density of 2.0 mA/cm^2, respectively. Fig.7B shows the GCD curves of supercapacitors based on PGOSAP hydrogel as a function of current density. The specific capacitance of the supercapacitor based on PGOSAP hydrogel was about 1.5 F cm^{-2}, 1.2 mF cm^{-2}, 1.1 F cm^{-2}, 0.9 F cm^{-2} and 0.7 F cm^{-2} at 1.0 mA/cm^2, 1.4 mA/cm^2, 2.0 mA/cm^2, 3.0 mA/cm^2 and 4.0 mA/cm^2, respectively. Although the current density has increased by 4 times, the area

capacity retention dropped by about 50%. When the current density increased from 1.0 to 4.0 mA/cm^2, the area energy density of supercapacitor slightly decreased from 0.154 to 0.039 mWh/cm^2 in the range of area power density from 613.8 and 286.8 mW/cm^2. As shown in Table 1[8, 23-26], the present supercapacitor shows the largest area special capacity and area energy density in comparison with others supercapacitors based on PANI and GO reported in previous literature.

Table 1. Data of previous SA/PANi or PVA/PANi based reports compared with our work.

Composite materials	Specific Capacitance	Substrate	Reference
PANI/PAAm	0.14 F/cm^2 (supercapacitor)	NO	[8]
PVA/PANI	302 F/g (electrode)	NO	[23]
SA/PANI	252 F/g (electrode)	Stainless steel mesh	[24]
PVA/PANI	0.31 F/cm^2 (supercapacitor)	NO	[25]
PVA/PANI	0.31 F/cm^2 (supercapacitor)	Carbon cloth	[26]
PVA/SA/PANI	1.5 F/cm^2 (or 613.8F/g) (supercapacitor)	NO	This work

The flexibility of the present supercapacitor based on PGOSAP was also evaluated as shown in Fig.8. It clearly showed similar CV curves for supercapacitor based on PGOSAP after multiple-time folds (Fig.8A). At the same time, the GCD curves of supercapacitor based on PGOSAP was characterized as a function of fold (Fig.8B). After multiple-time folds, the GCD curves were slight change. It also showed similar specific capacity of 877.3 mF cm^{-2}, 877.3 mF cm^{-2}, 864.9 mF cm^{-2} and 857.3 mF cm^{-2}, corresponding to bending angles of 0° , 90° , 180° and 360° , respectively. The capacitance of flexible supercapacitors remained almost unchanged under different bending angles. This result again proves the good flexibility of the supercapacitor based on PGOSAP. The good flexibility of supercapacitor was attributed to good flexibility and mechanical stability of electrode based on PGOSAP hydrogel. The cyclic stability of the supercapacitor based on PGOSAP hydrogel was further evaluated as shown in Fig.8C. At a current density of 3.0 mA/cm^2, capacity retention rate of up to 74.5% after 3500 charge/discharge cycles, showing outstanding cyclic stability. Furthermore, the strong interface between electrode (PGOSAP hydrogel) and electrolyte (H_2SO_4/PVA) was also key role for the good flexibility of supercapacitor (Fig.8D). There have no displacement or delamination between the interfaces. This experiment provides reliable technical support for flexible stretchable supercapacitors and is expected to become an energy supply equipment for a new generation of stretchable electronic products.

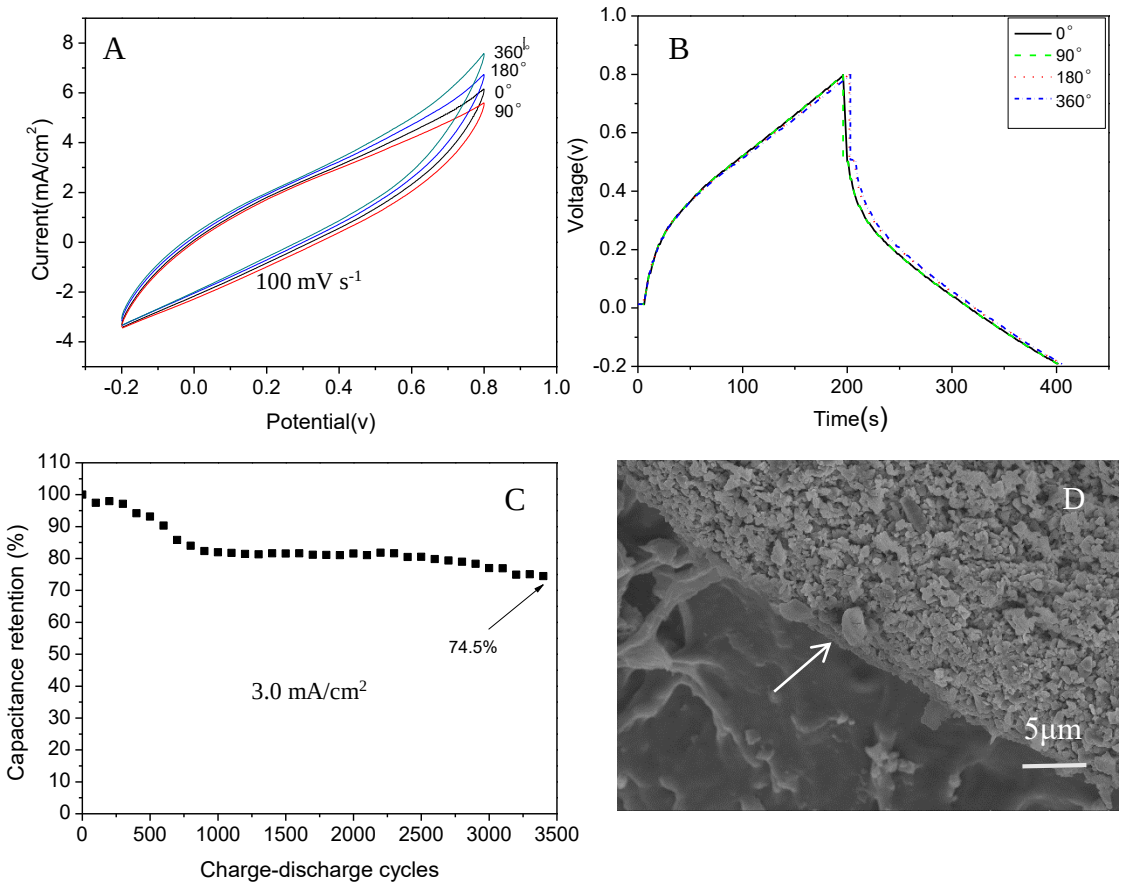

Figure 8. (A) CV curves and (B) GCD curves of supercapacitor based on PGOSAP hydrogel at different bending angle. (C) Cycling stability of supercapacitor based on PGOSAP hydrogel. (D) SEM image of interfacial contact in the supercapacitor after 3500 test cycles.

Fig.9 shows the electrochemical impedance spectroscopy of supercapacitors based on PGOSAP and GOSAP hydrogel from 0.01 to 100 KHz. The equivalent series resistance (ESR) of supercapacitors based on PGOSAP and GOSAP was about 2.9 Ω and 3.7 Ω, respectively. The lower ESR indicated lower internal resistance and lower charge transfer resistance, indicating enhanced electrochemical performance. The result can be attributed to good conductivity of graphene and improve interfacial contact between hydrogel electrode and current collector. The ability of electrolyte to conduct current is based on the directional migration of charged solvated ions between two electrodes under the action of electric field[27]. Therefore, the channel between electrolyte and electrode is the key point of ion directional movement. The internal resistance of PGOSAP hydrogel is relatively lower, which is related to the hierarchical network structure of PGOSAP hydrogel and its good compatibility with electrolytes. Meanwhile, the semicircle in the high-to-medium frequency region was also observed for the supercapacitors based on PGOSAP and GOSAP. The diameter of supercapacitors based on PGOSAP and GOSAP was about 2.1 Ω and 5.3 Ω, respectively. This result indicates a low ion diffusion resistance. In addition, the nearly vertical straight line in the low frequency region shows that the test system has strong capacitance characteristics, indicating that electrolyte ions can fully infiltrate the internal pores of the electrode material to form enough effective electric double layers, so that it has excellent capacitance performance.

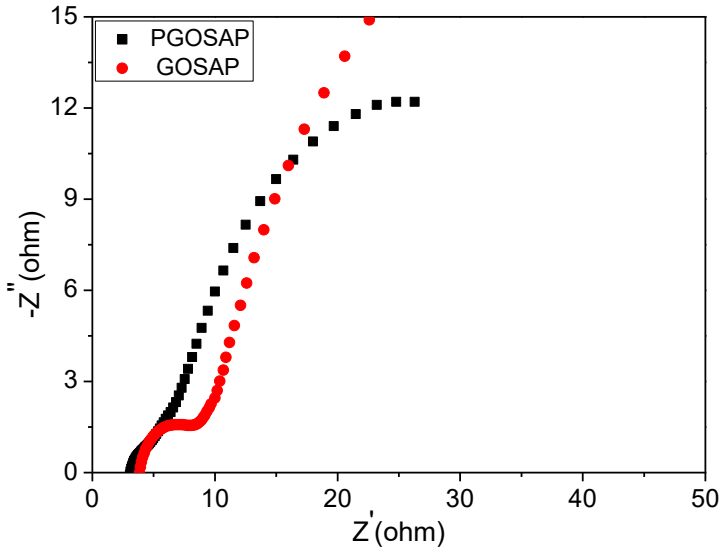

Figure 9. EIS spectra of supercapacitors based on GOSAP and PGOSAP hydrogel.

4. CONCLUSION

A new conductive hydrogel based on PVA, GO, SA and PANi was designed and prepared. The shape of hydrogel remained 1:1 with mold, and the conductive hydrogel has excellent mechanical stretchability. In addition, one-piece integrated flexible supercapacitor that does't need any additional elastic substrate as the overall stretchable electrode material was assembled based on PGOSAP hydrogel. The experimental results show that the electrolyte and electrode wich prepared all based on PVA have good compatibility, the assembled one-piece supercapacitor has no displacement and split-layer after 3500 GCD cycles.

CONFLICTS OF INTEREST:
There are no conflicts to declare.

ACKNOWLEDGEMENTS
The authors are grateful for the support of the Shanxi science and technology innovation project (202010D091), Applied research project of Yuncheng University (CY-2019029), and Doctoral research start project (YQ2020006).

DATA AVAILABILITY:
All data included in this study are available upon request by contact with the corresponding author.

References

1. Y. Zou, C. Chen, Y. Sun, S. Gan, L. Dong, J. Zhao and J. Rong, *Chem. Eng. J.*, 418 (2021) 128616.
2. T. Xu, D. Yang, S. Zhang, T. Zhao, M. Zhang and Z.Z. Yu, *Carbon*, 171 (2021) 201.
3. S. Sardana, A. Gupta, A.S. Maan, S. Dahiya, K. Singh and A. Ohlan, *Indian. J. Phys.*,96 (2022) 433.

4. Z. Wang and Q. Pan, *Chem. Electro. Chem.*, 9 (2016) 1407.
5. G. Qu, J. Cheng, X. Li, D. Yuan, P. Chen, X. Chen, B. Wang and H. Peng, *Adv. Mater.*, 28(2016) 3646.
6. Y.S. Zhang and A. Khademhosseini, *Science*, 356 (2017) 6337.
7. G.P. Hao, F. Hippauf, M. Oschatz, F.M. Wisser, A. Leifert, W. Nickel, N. Mohamed, Z. Zheng and S. Kaskel, *Acs. Nano*, 8 (2014) 7138.
8. H. Wang, L. Dai, D. Chai, Y. Ding, H. Zhang and J. Tang, *J. Colloid Interface Sci.*, 561 (2020) 629.
9. T. Guo, D. Zhou, W. Liu and J. Su, *Sci. China Mater.*, 64 (2020) 27.
10. K. Wang, X. Zhang, C. Li, X. Sun, Q. Meng, Y. Ma and Z. Wei, *Adv. Mater.*, 27 (2015) 7451.
11. X.J. Gao, Q.Z. Hu, K.J. Sun, H. Peng, X. Xie, H.A. Hamouda and G.F. Ma, *J. Alloy. Compd*., 888 (2021) 161554.
12. A. Gupta, S. Sardana, J. Dalal, S. Lather, A.S. Maan, R. Tripathi, R. Punia, K. Singh and A. Ohlan, *ACS Appl. Energ. Mater.*, 3 (2020) 6434.
13. J. Yang, X. Yu, X. Sun, Q. Kang, L. Zhu, G. Qin, A. Zhou, G. Sun and Q. Chen, *ACS Appl. Mater. Inter.*, 12 (2020) 9736.
14. B.S. Yin, S.W. Zhang, K. Ke and Z.B. Wang, *J. Alloy. Compd.*, 805 (2019) 1044.
15. G.Z. Guo, Y. Sun, Q. Fu, Y.B. Ma, Y.Y. Zhou, Z.Y. Xiong and Y.Q. Liu, *Int. J. Electrochem. Sci.*, 14 (2019) 5899.
16. G.Z. Guo, Y. Sun, Q. Fu, Y.B. Ma, Y.Y. Zhou, Z.Y. Xiong and Y.Q. Liu, *Int. J. Hydrogen Energy*, 44 (2019) 6103.
17. V.H. Nguyen, L. Tang and J.J. Shim, *Colloid Polym. Sci.*, 291 (2013) 2237.
18. H. Huang, J. Yao, Y. Liu, X. Tuo, Y. Da, X. Zeng and L. Li, *J. Macromol. Sci. B*, 56 (2017) 532.
19. P. Yang and W. Mai, *Nano Energy*, 8 (2014) 274.
20. A. González, E. Goikolea, J.A. Barrena and R. Mysyk, *Renew. Sust. Energ. Rev.*, 58 (2016) 1189.
21. J. Wang, J. Tang, Y. Xu, B. Ding, Z. Chang, Y. Wang, X. Hao, H. Dou, J.H. Kim, X. Zhang and Y. Yamauchi, *Nano Energy*, 28 (2016) 232.
22. F. Wu, X. Wang, S. Hu, C. Hao, H. Gao and S. Zhou, *Int. J. Hydrogen Energy*, 42 (2017) 30098.
23. R. Rajamany, S. Prakash and Y.A. Ismail, *Plast. Rubber. Compos.*, (2021) 1981090.
24. H.B. Huang, X.P. Zeng, W. Li, H. Wang, Q. Wang and Y.J Yang, *J. Mater. Chem. A,* 2 (2014) 16516.
25. R.F Hu and J.P Zheng. *J. Power Sources.*, 364 (2017) 200.
26. W.W Li, F.X. Gao, X.Q. Wang, N. Zhang and M.M Ma, Angew. *Chem. Int. Ed.,* 55 (2016) 1.
27. L. Dong, C. Xu, Q. Yang, J. Fang, Y. Li and F. Kang, *J. Mater. Chem. A*, 3 (2015) 4729